Journal of Intelligent & Robotic Systems (2024) 110:69
https://doi.org/10.1007/s10846-024-02080-9

REGULAR PAPER

A Bioinspired Control Strategy Ensures Maneuverability and Adaptability for Dynamic Environments in an Underactuated Robotic Fish

Gianluca Manduca[1,2] · Gaspare Santaera[1,2] · Marco Miraglia[1,2] · Godfried Jansen Van Vuuren[1,2] · Paolo Dario[1,2] · Cesare Stefanini[1,2] · Donato Romano[1,2]

Received: 8 November 2022 / Accepted: 28 February 2024 / Published online: 6 May 2024

Abstract
Bioinspired underwater robots can move efficiently, with agility, even in complex aquatic areas, reducing marine ecosystem disturbance during exploration and inspection. These robots can improve animal farming conditions and preserve wildlife. This study proposes a muscle-like control for an underactuated robot in carangiform swimming mode. The artifact exploits a single DC motor with a non-blocking transmission system to convert the motor's oscillatory motion into the fishtail's oscillation. The transmission system combines a magnetic coupling and a wire-driven mechanism. The control strategy was inspired by central pattern generators (CPGs) to control the torque exerted on the fishtail. It integrates proprioceptive sensory feedback to investigate the adaptability to different contexts. A parametrized control law relates the reference target to the fishtail's angular position. Several tests were carried out to validate the control strategy. The proprioceptive feedback revealed that the controller can adapt to different environments and tail structure changes. The control law parameters variation accesses the robotic fish's multi-modal swimming. Our solution can vary the swimming speed of 0.08 body lengths per second (BL/s), and change the steering direction and performance by an angular speed and turning curvature radius of 0.08 rad/s and 0.25 m, respectively. Performance can be improved with design changes, while still maintaining the developed control strategy. This approach ensures the robot's maneuverability despite its underactuated structure. Energy consumption was evaluated under the robotic platform's control and design. Our bioinspired control system offers an effective, reliable, and sustainable solution for exploring and monitoring aquatic environments, while minimizing human risks and preserving the ecosystem. Additionally, it creates new and innovative opportunities for interacting with marine species. Our findings demonstrate the potential of bioinspired technologies to advance the field of marine science and conservation.

Keywords Biorobotics · Biomimetics · Fish robot · Magnetic transmission system · Central pattern generators · Proprioceptive feedback control · Environmental robotics

1 Introduction

Underwater robotics is increasingly grabbing the attention in science and society for its role in exploring the unknown and delicate ocean environment. Underwater scenarios poses particular challenges to humans due to the difficulty of communication and the conflict between the importance of saving the aquatic ecosystem and human needs. Ocean, a fundamental resource for humans, covers much of the earth's surface and most of it remains unexplored [1]. Marine ecosystems provide food, produce oxygen, regulate the climate, and host rich biodiversity. Humans's ecological footprint is constantly growing and is damaging the balance of the ecosystems, including oceans, thus immediate actions are imperative [2]. Plastics [3] and heavy metals [4] are just two examples of the numerous pollutants that pose a significant threat to the health and well-being of the marine ecosystem. Robotics offers a variety of solutions, including towed systems, Human Occupied Vehicles (HOVs), Remotely Operated Vehicles (ROVs), and Autonomous Underwater

✉ Gianluca Manduca
gianluca.manduca@santannapisa.it

✉ Donato Romano
donato.romano@santannapisa.it

Extended author information available on the last page of the article

Vehicles (AUVs), which are employed to explore and monitor oceans with sustainable and robust approaches [5]. These technologies have the ability to reach significant depths [6], mitigating human risks and contributing to environmental conservation [7]. However, underwater robotics still faces significant challenges such as movement mechanics, sensory apparatus, and control strategies that need to be addressed.

The effective locomotion strategies evolved by aquatic animal species are an ever-increasing source of inspiration for the reproduction of efficient, and agile artifacts able to navigate in complex underwater areas. In a recent study, a tunable stiffness solution has been adopted to achieve high efficient swimming in a bioinspired artifact [8]. In addition, with the advent of soft-robotics, the use of pliant materials with low environmental impact is increasingly adopted. An instance of this is the proposal by Rossi et al. [9] which suggests utilizing shape memory alloys (SMAs) as a solution. Bioinspired robotic platforms have emerged as a powerful tool for testing and validating biological hypotheses, enabling breakthroughs in fields such as zoology and neuroscience. For instance, Tytell and Long [10] investigated the neuromechanical coordination of undulatory swimming, while Manfredi et al. [11] explored optimized swimming and goal-directed locomotion. These studies demonstrate the potential of bioinspired robotics to shed light on the underlying principles of biological systems and inspire new design solutions for robotic applications. Biomimetic design also allows scientists to develop agents capable of approaching living organisms with reduced stress in order to study and interact with them [12]. These robots have presented new opportunities for interaction with marine species, such as in the case of closed-loop systems, where robotic artifacts manage movement in response to the behavior of the specimens being studied [13]. Regrettably, the bulk of ethorobotics research has thus far been confined to controlled laboratory settings, with the prevalent utilization of decoys affixed to either stationary or mobile robotic platforms. Polverino et al. [14], for instance, employed this approach by swimming a controlled lure together with golden shiners (*Notemigonus crysoleucas*) in a water tunnel, to study their interaction. Similarly, Porfiri [15] exploited a small lure to study zebrafish social behavior and fear response. These robots have potential applications to improve animal farming conditions, preserve wildlife, and control pest species in both non-aquatic [16] and aquatic [17] environments within the agricultural industry.

The biodiversity found underwater is reflected in the design and control strategies of numerous marine bioinspired robots. For instance, researchers have developed diverse lamprey-like robotic platforms. Stefanini et al. [18] proposed a magnetic transmission system for a lamprey-like robot with rigid vertebrae. This was done in collaboration with neuroscientists to validate biological hypotheses regarding locomotion control aspects [19]. Differently, Liu et al. [20] proposed a soft-body lamprey-like robot with flexible and compliant sensors. In other studies, the propulsion system based on the pectoral fin of the manta ray has been explored, evaluating its efficiency through various fin shapes [21] and thicknesses [22]. Among the different locomotion strategies in aquatic environments, carangiform and subcarangiform swimmers can reach high speed ranges lowering the maneuverability to anguilliform swimmers due to fewer degrees of freedom. The body undulation, in this case, is localized mainly in the rear part while maintaining the major part of the anterior portion rigid. Different approaches have been adopted to achieve such bioinspired movements. Usually, the actuation system is composed of different motors coupled with the tail fin in different ways. Essex MT1 robotic fish [23] exploits two R/C servo motors and fifteen metal shafts to achieve tail and pectoral fin movements. Also, FIsho [24] used two different servo motors placed side by side in the head to actuate two joints. In Nanyang Arowana-like fish (NAF) [25], two micromotors have been considered to actuate a three- joints system. The robot proposed in [26] exploits 5 DC motors with a caudal fin made of wood laminates and pectoral fins made of cast epoxy. In [27], a single motor propels three rigid links through an eccentric wheel. The application of magnetic transmission proves to be a robust, simple, and reliable method. Notably, this technique allows for isolating moving parts from the main structure, enhancing impermeability. Moreover, the integration of a non-blocking magnetic mechanism reduces the risk of motor overload, particularly when the tail encounters obstacles. This actuation technique has been explored in various research scenarios, encompassing both multi-link actuated robotic models [18] and underactuated configurations [28].

Underactuated solutions allow the reproduction of complex movements improving the system reliability, decreasing the overall load, and saving energy. Marine species not only inspire the design choices but also in control aspects. CPGs are responsible for locomotor activity in vertebrates and invertebrates. They are neuronal circuits that can produce rhythmic motor patterns without sensory or high-level inputs carrying specific timing information [29, 30]. Most of the solutions which rely on these networks to control the locomotion of bioinspired robotic artifacts exploit multi-link systems independently actuated [31–33] instead of exploiting underactuated solutions, as proposed in [34]. Studies involving CPGs for locomotion control open the door to solutions that can move dexterously even in complex environments such as the marine for environmental monitoring and interaction with the ecosystem, as in the above-mentioned work [19] but also as proposed in [35]. To achieve motor patterns that can adapt to the environment, the integration with sensor inputs is essential [36]. CPGs can benefit from proprioceptive sensing, thus introducing a feedback control strategy for pattern modulation. For instance, in fish, this approach has been shown to

result in significant energy savings, as demonstrated through testing with a robotic solution in [37]. Additionally, proprioceptive control has been successfully validated in [38] using an underactuated robotic fish. This strategy offers a useful tool for developing robust and efficient bioinspired swimming solutions. Overall, incorporating proprioceptive sensing into CPGs can lead to improved performance and energy efficiency, making it a promising avenue for future research in this field.

Here we propose a novel control strategy for an underactuated robotic fish. The robotic artifact is inspired by pelagic fish and exploits only one DC motor to reproduce the caringform swimming mode. It is characterized by a modular and biomimetic design, with a transmission system that resembles the contraction and relaxation of the lateral tail muscles. The solution combines a magnetic coupling and a wire-driven mechanism to convert the oscillating movement of the motor into an oscillatory motion of the robotic fishtail. A proper bioinspired control strategy allows for exploiting the advantages of a modular and underactuated solution with a non-blocking transmission system. The approach results in muscle-like control based on CPGs. The proprioceptive feedback integration allows for investigating the adaptability of the control strategy under different environments and design configurations. The maneuverability of the underactuated robotic platform has been proven through different tests. Energy consumption was evaluated according to the design choice and control law adopted. The main contribution of this work is the development of a bioinspired control strategy that renders effective a solution based on a magnetic coupling system to reproduce a fish-like movement through a robotic artifact with a single motor. Thanks to the proposed control strategy, the robot can turn and vary its swimming speed, adapting its tail beat to different environments and configurations through proprioceptive feedback. The remainder of this research is organized as follows: First, the robotic fish's model, structure, and mechanism are presented. Second, the developed control strategy is explained. Then, experimental results to prove and validate the control strategy are shown and discussed.

2 Materials and Methods

2.1 Modeling, Structure, and Mechanism

Underwater robotics is a key tool for environmental parameters monitoring and exploration missions. Fish robots reproduce the aquatic species efficient and energy saving movements to swim with agility even in complex underwater environments. The bioinspired robotic fish developed takes pelagic fish as biological reference and it generates the thrust by bending its body into a propulsive wave that extends back to its caudal fin. Figure 1 shows the artifact structure, the working principle of the transmission system, and the reference systems.

The robot swims with the carangiform mode, a body-caudal fin (BCF) locomotion which can be described as an amplitude-modulated traveling wave [39, 40]. The following equation models the imposed transverse motion in a body-fixed coordinate system for carangiform robotic fish [41]:

$$y_t(x_t, t) = (c_1 x_t + c_2 x_t^2) \sin(k x_t - \omega t), \tag{1}$$

where y_t and x_t are the sideward and axial displacement, respectively, in the coordinate system $\{S_t\}$ in Fig. 1(B) while t denotes the time. $k = 2\pi/\lambda$ is the wave number, λ represents the wavelength, while ω is the circular frequency of oscillation. c_1 and c_2 are the wave amplitude's linear and quadratic coefficients, respectively. The last two parameters can be adjusted to achieve the desired BCF swimming mode.

Lighthill introduced the Elongated Body Theory in 1960 [42], which gained widespread acceptance for analyzing the hydrodynamics of elongated fish locomotion and propulsion efficiency [43–47]. The fish can achieve a steady state and maintain a constant mean speed, denoted by U, when the force generated by its thrust equals the opposing drag force. In this context, the average is taken over one period of the fish's body undulation. This concept is fundamental to the study of fish locomotion, and Lighthill's Elongated Body Theory can be used to calculate the mean thrust required to maintain this steady state speed, described as:

$$\overline{T} = \left[\frac{m}{2} \left(\overline{\left(\frac{\partial y(x,t)}{\partial t} \right)^2} - U^2 \overline{\left(\frac{\partial y(x,t)}{\partial x} \right)^2} \right) \right]_{x=l}, \tag{2}$$

where $\overline{(\cdot)}$ expresses the mean value, l denotes the length of fish, and m is the virtual mass, described as:

$$m = \frac{1}{4} \rho \pi S_c^2 \beta, \tag{3}$$

where ρ is the fluid density, S_c is the width of tail at $x = l$, and β is the coefficient of virtual mass correction, a non-dimensional parameter close to the value of one. Under conditions of inviscid flow, a cruising fish will experience a drag force, expressed as:

$$F_D = \frac{C_D \rho U^2 S}{2}, \tag{4}$$

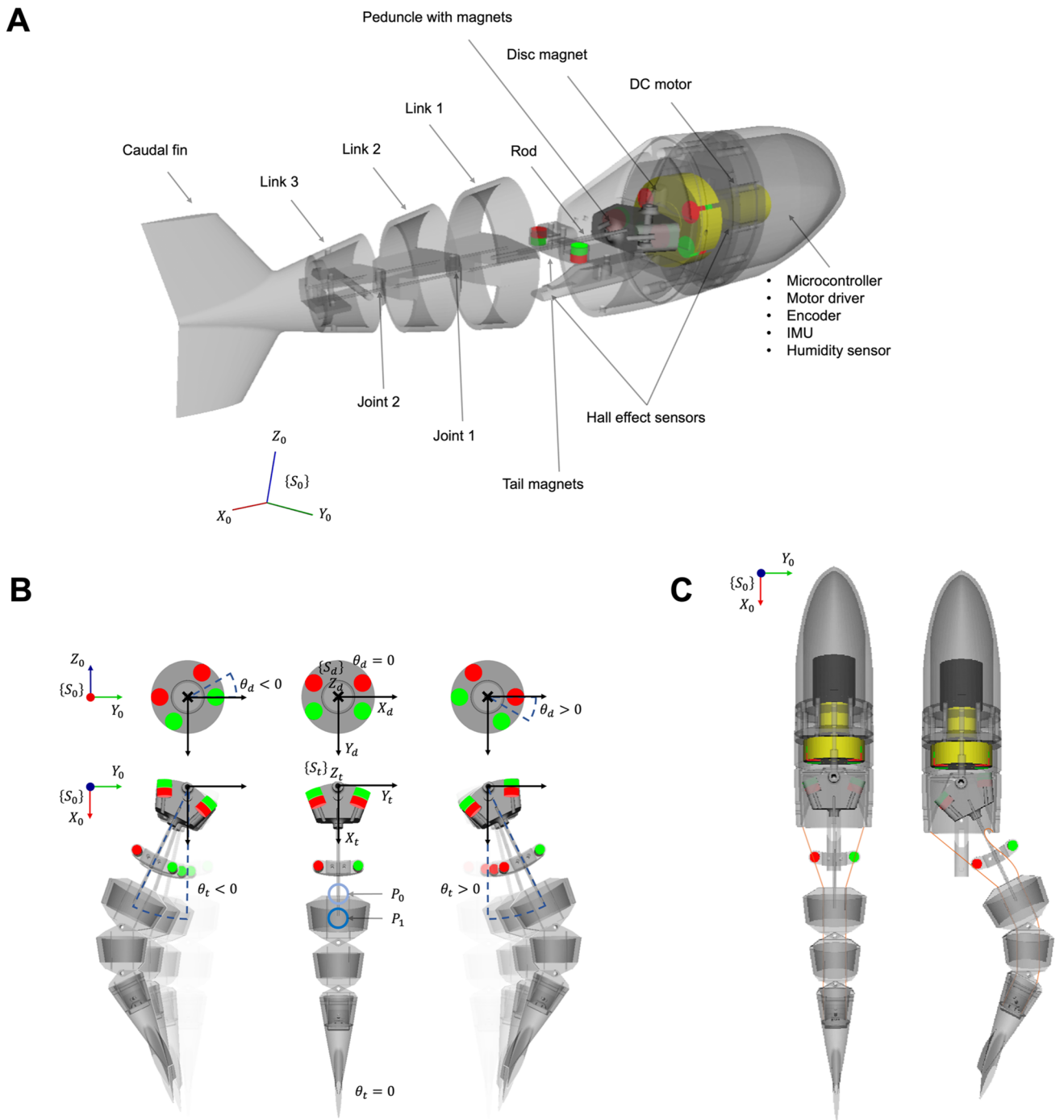

Fig. 1 Robotic fish design: (**A**) Structure representation with the related components description. (**B**) Visual description of the magnetic transmission mechanism with the reference coordinate systems considered. (**C**) Representation of the wire mechanism

and a resulting drag moment, expressed as:

$$M_D = -K_D \omega^2 sign(\omega), \tag{5}$$

where C_D and K_D are the drag force and moment coefficients, respectively, S is the wet surface area of the undulating body part, and ω is the angular speed. Once the fish achieves a balance between thrust and drag forces, we can calculate its U speed as follows:

$$U = \left[\sqrt{\frac{m\overline{\left(\frac{\partial y(x,t)}{\partial t}\right)^2}}{C_D \rho S + m\overline{\left(\frac{\partial y(x,t)}{\partial x}\right)^2}}} \right]_{x=l}. \tag{6}$$

The robotic platform consists of two main parts: a watertight head and an oscillating mechanism exposed to water. The head contains all necessary electronics, while the oscillating mechanism consists of a peduncle, a rod, three links, two joints, and a final caudal fin inserted into the final link, as seen in Fig.1(A). The proposed artifact utilizes only one DC gear motor to reproduce the bioinspired locomotion presented above. The system transforms the oscillating movement of the DC motor into an oscillatory motion in the robotic fishtail through the combination of a magnetic coupling and a wire-driven mechanism, illustrated in Fig. 1(B) and (C). A motor located in the head imparts an oscillating motion to a plastic disc containing four inserted permanent magnets (disc magnet). The arrangement and orientation of these magnets divide the disc magnet into two regions with opposing polarities. In the peduncle, two magnets face the disc-side with the same polarity. Contactless mechanical power transmission results from attractive/repulsive forces between the disc magnet and peduncle magnets. The peduncle connects to the first link using a rod, forming a system which we refer to as oscillating arm, and all links are interconnected in movement through hinges and a wire system, as depicted in Fig. 1(C). Each link incorporates two channels parallel to the mid-axis of the fish (on both sides) for the wires to pass through. The wire system connects the three links and the caudal fin to the head. When the magnets on the disc attract one of the magnets in the peduncle, the other is repulsed. Consequently, the oscillating rod bends towards the attracted magnet, and the tail tip points to the side of the repulsed magnet, following the wire system. The absence of any mechanical connection between the motor shaft and the oscillating arm ensures a non-blocking transmission system, preventing damage to the DC motor and the entire structure from overloading.

The mechanical design of the robot is an evolution of a previous artifact that was developed in our laboratory at The BioRobotics Institute of Scuola Superiore Sant'Anna (Pisa, Italy) [28], and it presents several modifications. With the previous version of the robot, the non-blocking transmission system was validated. Only a DC motor was contained, while the electronics were excluded from the body. However, in this work, the size of the robot was increased. The actual robotic fish weighs 875 g, and when $\theta_t = 0$ rad, it has a length from head to tail tip of 40 cm. This is unlike the first version, which had a weight of 77 g and a length of 17.9 cm. In this new version, the motor driver, a microcontroller, together with a sensor apparatus comprising a quadrature encoder, Hall effect sensors, an inertial measurement unit (IMU), and a humidity sensor were incorporated into the robotic artifact. In accordance with the increased size of the robot, different magnets and a different motor size were considered. The actuation mechanism underwent several changes aimed at ensuring control of the robotic tail beat. Specifically, two modifications were made: first, the motor's unidirectional rotation in the previous version was replaced with a back-and-forth solution in the current version. Second, the configuration of the magnets inserted in the disc magnet was changed.

The position of the disc magnet θ_d determines the magnetic attraction/repulsive force exerted on the tail and, therefore, its torque. The force values have been experimentally measured with different disc magnet/tail configurations through a dynamometer placed in P_0 (Fig. 1(B)). Figure 2(A) shows the results converted into torque values.

Bipolar Hall effect sensors are an effective solution for the absolute measurement of the disc magnet position, according to the small size and robustness to disturbances. Figure 2(B) shows the the signal received during magnets rotation. Two Hall effect sensors improve the system reliability and they allow the detection of direction changes. An IMU sensor with 9 DoF is placed inside the fish robot head while a quadrature encoder, integrated on the motor shaft, provides data on the shaft's relative position, speed, and acceleration. In this study, two Hall effect sensors, measure the magnetic field of the disc magnet, and they set the reference position $\theta_d = 0$ rad (Fig. 1(B)) during an initial setting phase. The quadrature encoder measurement is relative to it. The encoder is therefore responsible for measuring the position of the disc magnet during the control phase. Another Hall effect sensor measures the magnetic field of two magnets connected to the tail. The magnetic field value is converted into the tail angular position. The curve relating the tail angular position and the sensor measurements has been characterized by interpolation through the Curve Fitting Tool of the MATLAB (MathWorks Inc., MA) software. Different functions have been evaluated. A second-degree polynomial fits the extrapolated data by considering two different sets of parameters according to the θ_t angle sign (Fig. 2(C)):

$$\theta_t(x_h) = ax_h^2 + bx_h + c, \tag{7}$$

where x_h is value in Volt read from the Hall effect sensor. Fig. 3 exhibits the finally assembled robotic fish.

2.2 Control Strategy

In this work, we investigated a muscle-like control for the developed robotic fish. The locomotion management by CPGs inspires the control strategy. The CPGs are networks that coordinate various motor patterns in vertebrates and invertebrates [29]. They are distributed in different areas of the nervous system, thus generating a rhythmic activity to consent complex movements. Similarly, the proposed control strategy produces a rhythmic oscillating activity in the motor, leading to a tail oscillation.

First, the stability of the proposed structure was analyzed. The system presented can be described as a DC motor mechanically coupled to a load (disc magnet) which interacts

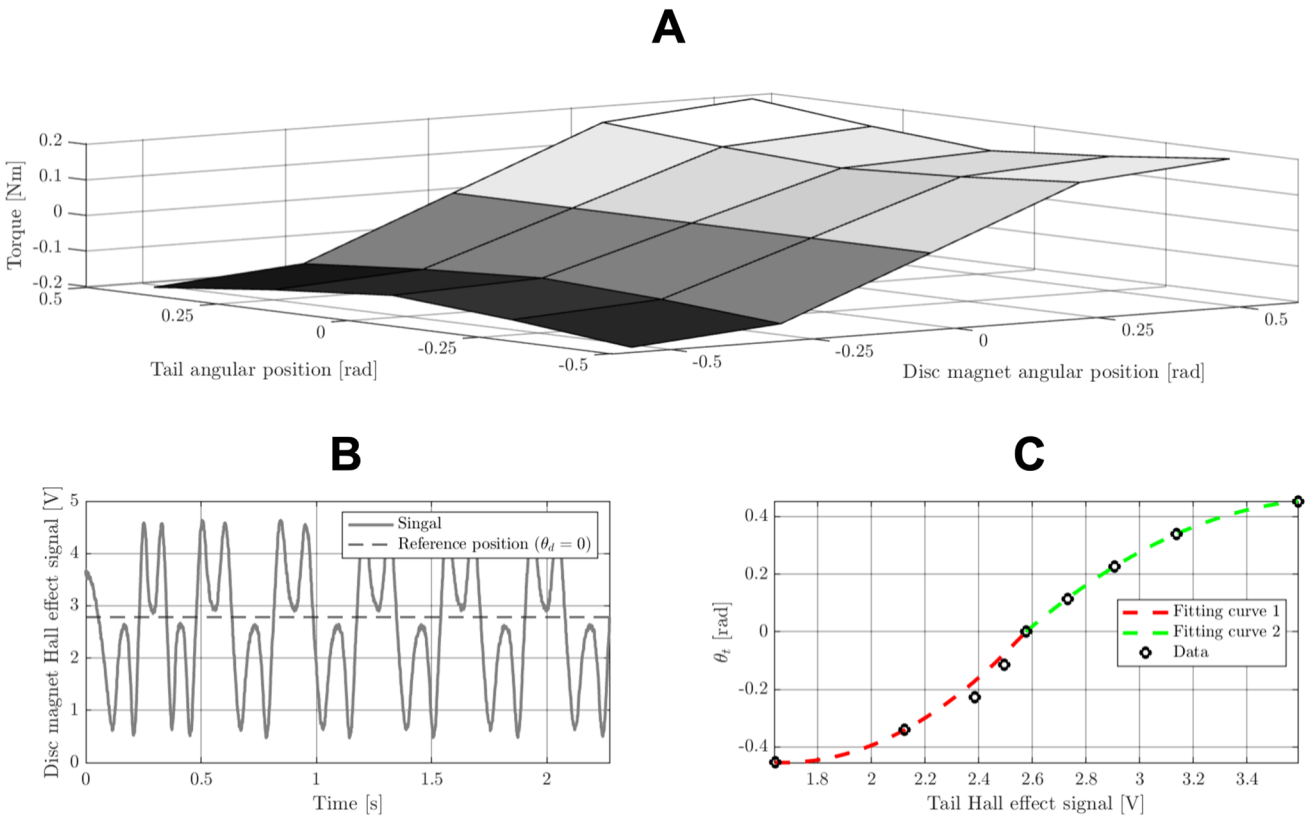

Fig. 2 Structure charachterization: (**A**) Torque exerted on the tail by the magnetic coupling between disc magnet and oscillating arm magnets according to different disc magnet/tail configurations. (**B**) Disc magnet Hall effect sensor signal received to set the reference position at θ_d = 0 rad. (**C**) Tail angular position characterization from the Hall effect sensor signal placed along the tail

through a magnetic coupling with an oscillating arm. To verify the stability of the system, a descriptive MATLAB model of the system to be controlled was created and the transfer function obtained was evaluated. The DC motor model can be described with the following equations [48]:

$$V_a(t) = R_a I_a(t) + L_a \dot{I}_a(t) + K_b \omega_p(t), \tag{8}$$

$$K_t I_a(t) = J_p \dot{\omega}_p(t) + D_p \omega_p(t) + \tau_l. \tag{9}$$

The variables and parameters of the motor's equations are described in Table 1, along with the parameters' adopted values.

The disc magnet angular position corresponds to the rotor one ($\theta_d(t) = \theta_p(t)$). The disc magnet and the oscillating mechanism were modelled as loads on the motor. The load torque was therefore expressed as follows:

$$\tau_l(t) = J_l \dot{\omega}_p(t) + A_l \sin(\theta_p(t)). \tag{10}$$

J_l represents the inertia of the disc magnet (0.000016 kg·m^2). The load resulting from the interaction between the disc magnet and the oscillating arm has been modeled as a sinusoidal disturbance, dependent on the rotor's position $\theta_p(t)$, with amplitude A_l. The value of this parameter (0.2 N·m) was chosen to match the maximum transverse torque in absolute value measured experimentally and depicted in Fig. 2(A). This choice represents the worst-case scenario

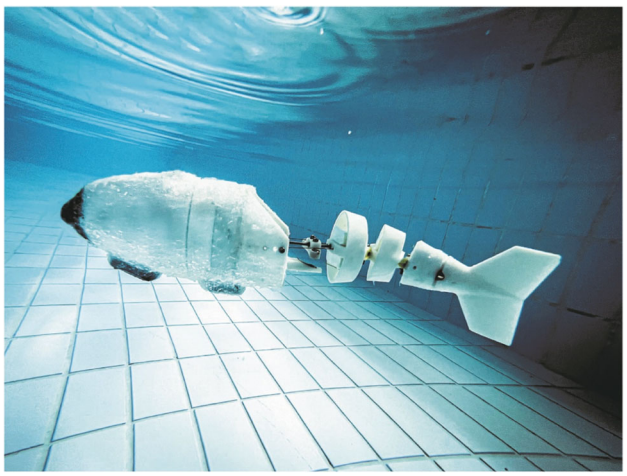

Fig. 3 Representative image of the finally assembled robotic platform during tests in a swimming pool

Table 1 Description of motor variables and parameters, along with their values used in the simulation

Variables and parameters	Description	Adopted values
$V_a(t)$	Armature voltage (V)	
$I_a(t)$	Armature current (A)	
$\omega_p(t)$	Rotor speed (rad/s)	
$\tau_l(t)$	Load torque $(N \cdot m)$	
R_a	Armature resistance (Ω)	4
L_a	Armature inductance (H)	0.000000610
K_b	Back emf constant $(V \cdot s/rad)$	0.2
K_t	Torque constant $(N \cdot m/A)$	0.2
J_p	Rotor inertia $(kg \cdot m^2)$	0.001
D_p	Damping constant $(N \cdot m \cdot s/rad)$	0.00025

since the tangential torque value, expressed by A_l, is lower in absolute value.

The open-loop function G_{ol} of the system was derived using MATLAB's *linmod* function from the model developed in Simulink:

$$G_{ol} = \frac{3.6 \cdot 10^8}{s^3 + 6.6 \cdot 10^6 s^2 + 8 \cdot 10^7 s + 1.3 \cdot 10^9}. \tag{11}$$

Then, the closed-loop transfer function G_{cl} was obtained as:

$$G_{cl} = \frac{G_{ol}}{1 + G_{ol}}. \tag{12}$$

Zeros and poles of the closed-loop transfer function are collected in Table 2. The feedback loop is stable since all poles have negative real parts.

A motor position control, which has a sinusoidal profile as a reference, generates rhythmic tail activity. In nature, CPG circuits determine the appropriate set of activation of the muscles without requiring feedback from the sensors. Motion management, in this sense, resorts to a feedforward control, thus ensuring the exact torque to achieve goal-directed motion at certain speeds [30, 49]. Incorporating proprioceptive sensing allows for the adaptation of rhythmic activity management [50]. This approach can further enhance the adaptability to different environments [51]. In the proposed control, the oscillatory reference integrates with proprioceptive sensory feedback coming from the tail. Figure 4(A) elucidates the core principle behind this control strategy. This approach controls the torque exerted on the fishtail by using a parameterized control law. This law takes the tail angle θ_t as input and determines the torque exerted on the fishtail. The reference torque is then converted into the corresponding configuration of the disc magnet. The control law is composed of three contributions. The first contribution is given by:

Table 2 Zeros and poles of the closed-loop transfer function

Zeros	Poles
$-6.5574 \cdot 10^6$	$-6.5574 \cdot 10^6$
$-5.1686+13.0455i$	$-6.5574 \cdot 10^6$
$-5.1686-13.0455i$	$-5.1686+14.8125i$
	$-5.1686-14.8125i$
	$-5.1686+13.0455i$
	$-5.1686-13.0455i$

$$\tau_{t,1}(\hat{\theta}_t) = k_1 sign(\dot{\hat{\theta}}_t)(1 - |\hat{\theta}_t|), \tag{13}$$

where $\hat{\theta}_t$ is the tail angle θ_t divided by its maximum value, resulting in $\hat{\theta}_t \in [-1.1]$. This contribution generates a torque that varies its sign according to the direction of rotation of the oscillating arm and is maximum in absolute value when the tail is at $\hat{\theta}_t = 0$. This contribution becomes null when the tail reaches the limit switches ($\hat{\theta}_t = \pm 1$). k_1 is a positive parameter. Increasing the value of k_1 results in a higher torque and, consequently, a higher oscillation frequency of the tail. The second contribution of the control law plays a crucial role in guaranteeing a call-back to the tail when it reaches the limit switches. This contribution opposes the effect of $\tau_{t,1}(\hat{\theta}_t)$ and is expressed as follows:

$$\tau_{t,2}(\hat{\theta}_t) = -k_2 \hat{\theta}_t, \tag{14}$$

where, in contrast to $\tau_{t,1}(\hat{\theta}_t)$, it has maximum and minimum peaks when the tail reaches the limit switches, and it cancels out when the tail is at $\hat{\theta}_t = 0$. The positive parameter k_2 defines the torque value imparted to the tail when approaching limit switches, countering the motion and changing the direction of rotation of the oscillating arm. k_2 is imposed to be smaller than k_1. If not, the control would reduce the torque when the oscillating arm begins its movement again after changing direction of rotation. This strategy reduces the loads on the motor resulting from the magnetic coupling between the tail and the disc magnet. The motor's controlled oscillation encounters a reduced tangential force. The third contribution of the control law generates a steering manoeuvre. It generates an asymmetry in $\tau_{t,1}(\hat{\theta}_t)$, increasing the torque value towards one direction of rotation of the oscillating arm while decreasing it towards the other. This contribution is expressed as follows:

$$\tau_s(\hat{\theta}_t) = k_s(1 - |\hat{\theta}_t|). \tag{15}$$

The sign of k_s determines the direction of curvature. The parameter's absolute value controls the asymmetry of the tail beat. It's crucial to ensure that k_s doesn't reduce the impact

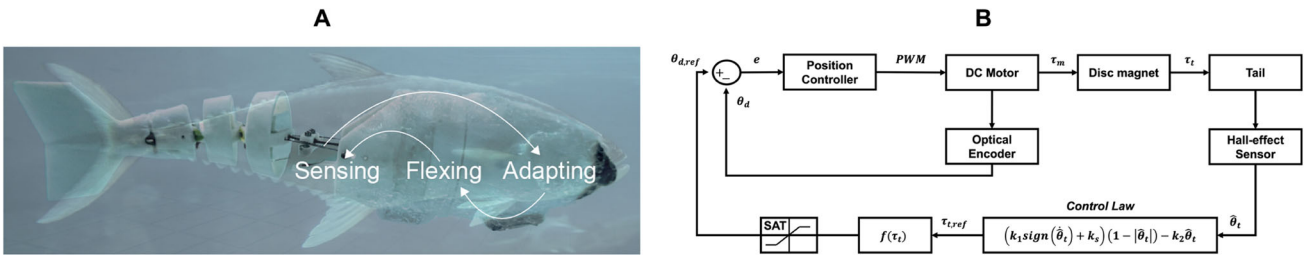

Fig. 4 Control strategy: (**A**) General description of the bioinspired approach. (**B**) Block diagram of the system

of k_1 to the point where k_1 becomes smaller than k_2, as previously mentioned. The control law is defined as the sum of the three contributions:

$$\tau_t(\hat{\theta}_t) = \tau_{t,1}(\hat{\theta}_t) + \tau_{t,2}(\hat{\theta}_t) + \tau_s(\hat{\theta}_t), \tag{16}$$

and it results in the following expression:

$$\tau_t(\hat{\theta}_t) = (k_1 sign(\dot{\hat{\theta}}_t) + k_s)(1 - |\hat{\theta}_t|) - k_2\hat{\theta}_t. \tag{17}$$

The following system collects the constraints to which the three parameters are subject:

$$\begin{cases} k_1, k_2 > 0 \\ k_1 > k_2 \\ (k_1 - |k_s|) > k_2. \end{cases} \tag{18}$$

The control law determines the reference torque corresponding to a particular disc magnet configuration according to the tail position. The relation between the torque contributed by the magnets and the disc magnet position was approximated by the following linear function:

$$\theta_d = k_{ln}\tau_t(\hat{\theta}_t). \tag{19}$$

θ_d is the angular position of the disc magnet (rad) according to the coordinate system $\{S_t\}$ (Fig. 1). The value of k_{ln} is determined by the system's maximum allowable torque and the disc magnet's angular operating range. By considering normalized torque values, the control law can be generalized. The choice of k_{ln} is then determined by the disc magnet's angular operating range, which is dictated by the spacing between the magnets in the disc. For the design presented, k_{ln} is set at 0.52. This means that when the torque is at its maximum value ($\tau_t(\hat{\theta}_t)$=1), the disc magnet's position corresponds to θ_d=0.52 rad. On the other hand, when the torque is at its minimum ($\tau_t(\hat{\theta}_t)$=-1), θ_d will be -0.52 rad. The overall strategy reduces to position control of the motor. The reference position tracking relies on a PID controller. A Pulse Width Modulation (PWM) strategy is adopted. Figure 4(B) shows the block scheme of the entire system. To prevent the system from overstepping the operating range of the disc magnet and nullifying the control strategy, saturation is taken into consideration.

To initiate the algorithm, the quantities that need to be defined are k_{ln}, k_1, k_2, k_s, and the PID parameters. Among these, k_{ln} is structural. k_2 determines the continuous oscillation of the system. k_1 and k_s are adjustable and can influence performance in terms of frequency and asymmetry of the oscillation, respectively. A key feature of this approach lies in its adaptability. The control strategy benefits from proprioceptive feedback to adapt to different situations. When changing the tail's structure, weight, or the environment in which the robotic fish operates, the controller adjusts accordingly. This is because the tail's position determines the motor's oscillating reference position. Otherwise, a predefined sinusoidal reference would require amplitude and frequency calibration for each context. A strategy without proprioceptive feedback, in fact, could result in the magnetic coupling breaking down. To visually explore our proposed artifact, control strategy, and the conducted tests, please refer to Video S1.

2.3 General Observations

The final CAD model of the robotic fish was developed into the commercial software Solidworks. Based on FDM technology, the robotic fish was manufactured with a Zortrax M200 3D printer. Z-ULTRAT material was used, an ABS-based plastic with superior mechanical properties to pure ABS. Only the cylinder connecting the motor shaft with the disc magnet was made in aluminum for more robust transmission. The DC motor sized for this work is a high-power, 6 V brushed DC motor combined with a 34.014:1 metal spur gearbox. A 48 CPR quadrature encoder is mounted on the motor shaft. The microcontroller board is an ESP32, while the motor driver is a VNH5019A, one-channel. The DC power supplier considered is an IPS2303. The neodymium magnetic discs sized for the robotic fish have a diameter of 12 mm, an height of 10 mm, and an holding force of 5.3 kg. The wire connecting the tail components with the robotic fish head has a diameter of 0.3 mm and it can hold up to 20 kg. All tests were carried out first in air and then in water. The water tank considered for testing is 1 m long and 0.5 m high.

Then the robotic fish and the various tests were repeated in a larger environment that is in a pool 10x5 m, deep 0.8 m. A global view camera is set above the swimming pool to record the movement of the robotic fish during the experiments. The data coming from the internal sensors have been saved on the internal memory of the microcontroller and then extrapolated and analyzed with the MATLAB software. The data were taken via Bluetooth at the end of each experiment. In the same way, the various parameters have been sent for the control strategy analysis and the evaluation of the relative performances. The control strategy has been implemented directly on the microcontroller. The firmware has been uploaded via Wi-Fi on the microcontroller without opening the head of the fish containing the electronics, avoiding any risk of damage during the experiments.

3 Results

Different tests have been conducted to validate the control strategy and proof its adaptability under different conditions. First, the control law has been validated, considering the robotic artifact stuck in the water. Figure 5(A) shows the fishtail and disc magnet angular position for a given set of parameters ($k_1 = 1, k_2 = 0.4, k_s = 0$). The data have been collected in the controller's internal memory and analyzed after the test. The selected set of parameters consists of the nominal condition, where there is no steering contribution. The call-back contribution considered is the minimum value empirically computed to ensure the proper functioning of the strategy, and k_1 is set to the maximum value to avoid saturation. The fishtail dictates the motor oscillation. The motor's oscillation drives the oscillation of the disc magnet. According to the related reference systems, the developed control law generates a phase shift between the disc magnet and fishtail angular positions. When the fishtail approaches the limit switches, the disc magnet configures in the angular position $\theta_d = 0$ rad. Thanks to the call-back contribution, the disc magnet configuration starts to push away the tail. Conversely, the magnets provide the maximum torque contribution in absolute value when $\theta_d = 0$ rad. Then, different tests were repeated, changing the external environment and increasing the weight of the fishtail. Figure 5(B) presents the change in the disc magnet oscillation and fishtail beating frequency according to different situations investigated. Frequencies were obtained with *plomb* MATLAB function by considering the maximum peak of the periodigram, and checked with the *Signal Analyzer* tool. The results compare the control performance of the robotic fish when suspended in air, submerged in water, and when additional loads are applied to the fishtail (in the water scenario). Two different weights, 0.075 kg and 0.140 kg were considered. The weights were positioned in P_1 (Fig. 1(B)) and they provide a constant torque disturbance of 0.0735 N·m and 0.1373 N·m, respectively. The fishtail and the disc magnet are magnetically coupled, and they oscillates with the same frequency. The results show a change in the oscillation frequency according to the different scenarios. The various scenarios emulate shifts in environmental conditions and alterations to the robot's structure. The fishtail, encountering constant disturbances during the beating, modulates the disc magnet oscillation according to the control law. This result shows the effectiveness of a closed-loop strategy. The controller can adapt to changes in shape, the weight of the tail, or liquid density in which the robotic fish swims, thanks to proprioceptive feedback. Otherwise, an open-loop strategy would result in a frequency invariation. For each scenario, the reference sinusoidal input would have to be defined. This would not only be time-consuming, but also less robust. In fact, if the tail gets stuck, the mechanical coupling could break. A break in the magnetic coupling can generate a tail beat that does not exploit the operating range, with a possible asymmetrical oscillation.

The non-zero value assigned to k_2 prevents the disc magnet from reaching the neutral position at the limit switches, ensuring continuous oscillation and avoiding tail stalling. This parameter was empirically selected to ensure proper func-

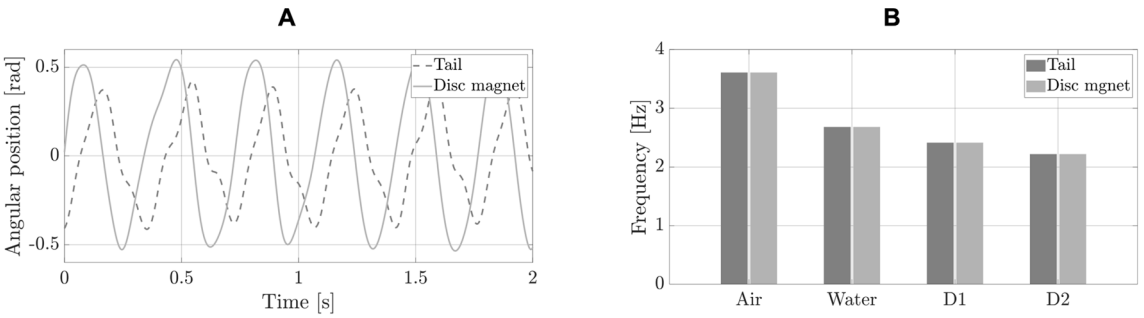

Fig. 5 Control strategy validation in nominal condition ($k_1 = 1$, $k_2 = 0.4$, and $k_s = 0$) with the robotic fish stuck: (**A**) Phase shift between the angular position of the tail (dashed line) and the disc magnet (solid line), test in water. (**B**) Tail beat and disc magnet change in frequency according to different environments (air - water) and different loads applied to the tail (D1 = 75 g, D2 = 140 g, water tests)

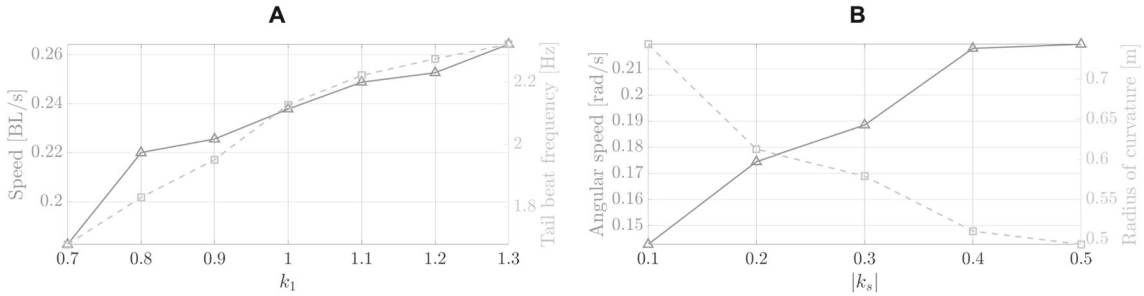

Fig. 6 Robotic fish performances according to the control parameters choice: (**A**) Change in tail beat frequency (dashed line) and the related robotic fish body speed (solid line) considering different values of k_1 with $k_2 = 0.4$, and $k_s = 0$, fixed. (**B**) Curvature radius (dashed line) and angular speed (solid line) varying the steering parameter k_s with $k_1 = 1$, and $k_2 = 0.4$, fixed

tionality of the strategy. Varying k_1 and k_s allows multi-modal swimming. Different tests have been carried on to evaluate the swimming performance changes related to these parameters. First, the fish body speed and the tail beat frequency have been investigated, varying k_1. No steering contribution was considered in this case ($k_s = 0$). The times to complete a predetermined distance were collected to measure the average fish body speed. In the following, the swimming speed of the robot will be indicated in body lengths per second (BL/s). The frequencies were analyzed as described above. Figure 6(A) shows the obtained results related to the parameter choice. The control law allows changing the torque exerted on the tail. Changing the torque exerted on the fishtail involves a frequency variation due to the magnetic transmission system. As expected, increasing the value of k_1 also increases the tail beat frequency and the fish's body swimming speed. According to the parameters evaluated, the tail beat frequency varies between 1.7 Hz and 2.3 Hz. The measured swimming speed change with the same trend between 0.18 BL/s and 0.26 BL/s. Differently, the parameter k_s allows changing the torque exerted on the fishtail according to the rotational direction of the oscillating arm. A change in torque with respect to the direction of rotation of the oscillating arm leads to an asymmetry in the tail beat. This parameter can influence the robotic fish's swimming direction and steering performances. Different tests have been carried maintaining fixed $k_1 = 1$ and let varying k_s. The steering performances have been investigated in terms of angular speed and radius of curvature. The parameter sign determines the steering direction, while its value changes the steering performance. Circular paths have been performed and both steering directions have been evaluated. Times and distances covered were obtained through a videos analysis. Figure 6(B) shows the change in the steering performances varying k_s. According to the control strategy, the robotic fish can increase/decrease the angular speed and the curvature radius. The steering performances increase with k_s absolute value. The robotic fish can improve the steering angular speed of 0.08 rad/s with a relative change in the curvature radius of 0.25 m. Figure 7 compares the robot steering performance with two different values of k_s through snapshots. The control strategy ensures a range of robotic artifacts' maneuverability despite its underactuated design.

Energy consumption is another essential feature for maintaining stable, proper, and long working conditions. The average current value with a DC motor power supply of 6 V is 0.2 A in the nominal condition. The Work Per Meter (WPM) represents the energy spent to travel a 1 m distance. It can be expressed as the ratio between the average electric power consumption P_{el} and the average swimming speed, resulting in WPM = 16.78 J/m. Another consumption index is the Cost of Transport (CoT), which consists of the energy consumption per unit distance and unit mass. It is simply equal to the ratio between the Work Per Meter and the mass of the robotic artifact. For the solution proposed it results CoT = 19.18 J/(kg·m).

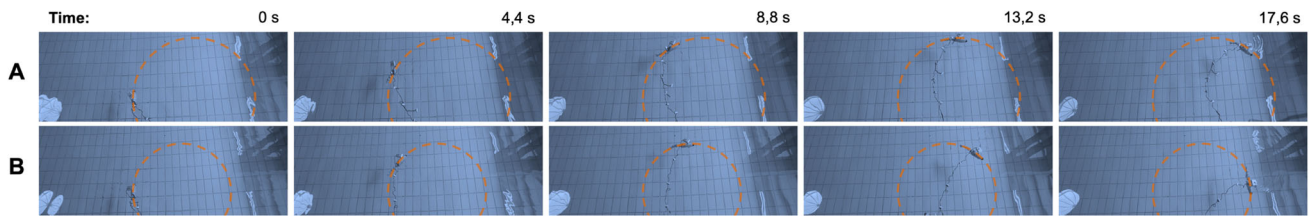

Fig. 7 Swimming pool experiments: Comparison through snapshots of steering performance change varying k_s in the control law with $k_1 = 1$, $k_2 = 0.4$ fixed. (**A**) $k_s = -0.1$. (**B**) $k_s = -0.3$

4 Discussion

Developing robust and sustainable robotic solutions for discovering and monitoring the marine ecosystem is essential. A bioinspired locomotion design and biomimetics allow acting in the harsh and unstructured ocean environment exploiting the agility and efficiency of the fish movements without causing stress to submarine species. The proposed solution combines a magnetic coupling and a wire-driven mechanism to convert the oscillating movement of one DC motor into an oscillatory motion of the robotic fishtail. The underactuated system improves the solution reliability and energy savings. Moreover, the non-blocking transmission system ensures waterproofness and prevents structure and actuating motor overload. The solution implemented is simple to manufacture and modular. A proper control strategy must guarantee the robotic fish's maneuverability to take advantage of this design choice.

The movement control in this study draws inspiration from CPGs, mimicking how fish activate muscles. Incorporating proprioceptive feedback into generating a sinusoidal reference position for the motor aims to enhance control robustness and adaptability across diverse environments and design configurations, distinguishing it from open-loop solutions. Results demonstrate the controller's adaptation to water and air conditions and varying tail loads. Across different environments and loads, the control system dynamically adjusts the tail beat frequency, exploiting the entire operating range and maintaining magnetic coupling. Additionally, speed and steering performance changes were observed by varying control law parameters, with swimming speed correlating with tail beat frequency. The curves illustrate a similar trend, reaching a maximum fish body speed of 0.26 BL/s with a 2.3 Hz tail beat frequency. The robotic fish developed here exhibits quite good performance as regards swimming speed according to the potential applications. These applications include approaching wild aquatic animals to monitor and interact with them in a minimal invasive way. So, a biomimetic and calm swimming artifact, without abrupt or too fast movements, would produce a lesser nuisance and aversion effect on living organisms compared to an artifact with better speed performance (this would reproduce a state of agitation or alertness in fish [52]). The steering performance of the robotic fish depends on two interdependent parameters - the angular speed and the radius of curvature. Based on various tests, two curves were empirically extrapolated. The fish can adjust its angular speed by 0.08 rad/s, resulting in a relative change in the radius of curvature of 0.25 m, showing high maneuverability. To further enhance speed and steering performances, options include employing magnets with stronger attraction/repulsion forces, modifying the motor size, or exploring different tail designs. The adaptable controller enables fish maneuverability, and the modular design facilitates improved swimming performance by modifying the fish's design while retaining the same control strategy.

This work is innovative on several fronts. The choice of the transmission system combines a magnetic non-blocking system with a wire-driven mechanism meant for a self-propelled robotic fish inspired at carangiform swimmers. Magnetic coupling systems have shown promise in actuating robotic platforms. Magnetic transmission presents a promising approach for achieving simple, robust, and reliable solutions. One of its benefits is the potential to separate moving parts from the rigid body, which can improve waterproofing. Additionally, the implementation of a non-blocking magnetic system can reduce the risk of motor overload if the tail gets stuck. However, when replicating nuanced fish-like movements, certain considerations arise. The inherent low rotational inertia of these systems can subtly differ from the natural, fluid undulations observed in living fish. Additionally, while offering consistent motion, the bandwidth of magnetic coupling might not always capture the rapid directional shifts typical in dynamic aquatic scenarios. Nevertheless, with careful design and control, these challenges can be mitigated, making magnetic coupling a viable choice for certain robotic fish applications. In literature, the use of a magnetic coupling system to reproduce a fish-like movement through a robotic artifact is not widespread. A similar transmission system has been exploited to investigate CPGs by reproducing a lamprey-like robotic fish [19]. In this case, however, the system is not underactuated, and it is composed of active and passive vertebrae that generates an anguilliform locomotion. In an other work, magnets couples two subsystems of a robotic platform for a direct underwater interaction study with small fish species [53]. More widespread instead is the wire-driven mechanism for the reproduction of underactuated and bioinspired solutions. For instance, PoTuna [54] and UC-Ika [55] use one motor mechanically connected to a system mechanism to mimic the tuningform movement. There are other examples which exploit only one motor with wires and a mechanical coupling for subcarangiform locomotion [56–58]. However, using an underactuated system and its advantages is not the first choice for developing bioinspired solutions. Most works exploit multiple motors to reproduce fish-like movements [23–25, 59, 60]. However, the actual innovative contribution of this work lies in the choice of a bioinspired and muscle-like control strategy that takes inspiration from CPG with the integration of proprioceptive feedback to make effective an underactuated and non-blocking solution. This approach allows exploiting an underactuated solution's advantages by guaranteeing the robotic fish's maneuverability and multimodal swimming. Most studies that exploit CPGs to control the movement of

fish-like robots use multi-link systems independently actuated, as in the case of i-RoF robotic fish [61], which exploits two different servomotors to activate its links. This control strategy is not always used among the various solutions underactuated [31–33]. In a similar study that involves a wire-driven underactuated system, it is demonstrated that with just one motor, the CPGs control can be easily implemented to obtain multimodal swimming [34]. Differently in our study, we integrated this feedforward control with the proprioceptive feedback to obtain an adaptable solution to the environment and structure. Similar to this integrated control strategy, in [38] force sense is used as input, differently from the tail position, and considering a mechanical coupling between the motor and fishtail. Considering the position of the tail is a robust choice. Also, the choice of a non-blocking system makes the solution more reliable to the various loads to which the robot can be subjected. The robotic fish head contains all the electronics, separated by the moving fishtail, for a more safe system. Those choices also consent to investigate the system mechanics and different fishtail configurations, which can be substituted easily, increasing performances, by maintaining the developed control strategy.

In this study, we employed a PID controller for reference position tracking. While this approach has demonstrated efficacy in our specific setup, it's worth noting that alternative control solutions might offer enhanced performance. While PID controllers are popular due to their simplicity and broad applicability, they have some inherent limitations. For instance, they may struggle with non-linear systems and require precise tuning. The emergence of learning controllers, such as those based on machine learning or adaptive control strategies, offers promising alternatives that can adjust and optimize in real-time [62–68].

Bioinspired and biomimetic robots have opened up new avenues for interacting with underwater species. However, the majority of ethorobotics research has been limited to laboratory settings where decoys, either stationary or mounted on mobile robotic platforms, have been predominantly used. [14, 15, 52, 69–71]. A free-swimming fish robot has been proposed for an animal-robot interaction study in [72]. Tests have also been carried out in the laboratory. To optimize its interaction with zebrafish, the robot's design has been specifically tailored, taking into account factors such as color pattern, aspect ratio, and tail beat frequency. The robot has been operated remotely using a control unit, and a servomotor located in the tail section has been used to actuate the body-tail joint and propelling the robot. In our work, we want to propose a robotic agent controlled independently of external robotic platforms, which could be used in this context and can be blended into animal populations. Although other robots have focused on biomimetic design, in our case we believe that this type of transmission would have a less disturbing effect on the populations of organisms being observed due to the magnetic coupling system, which would limit vibrations and noise produced by traditional mechanical drive systems.

5 Conclusion

This work investigated a muscle-like control for an underactuated robotic fish. The transmission system enables the control of the torque exerted on the fishtail. The control strategy is inspired by the CPGs and integrates proprioceptive feedback. According to a parametrized control law, the fishtail angular position dictates the reference torque. Several tests validated the proposed approach. The controller can adapt to changes in shape, the weight of the tail, or the liquid density in which the robotic fish swims. By varying the parameters, the control law can change the torque exerted on the tail. Changes to the torque involve a tail beat frequency variation due to the magnetic transmission system. Depending the parameters evaluated, the tail beat frequency can vary between 1.7 Hz and 2.3 Hz. The torque and the frequency variation dictate swimming speed changes. The swimming speed measured can vary between 0.18 BL/s and 0.26 BL/s. The solution also enables steering direction to be controlled along with the performance. The performances were evaluated in terms of angular speed and radius of curvature. The robotic fish can improve the steering angular speed of 0.08 rad/s with a relative change in the curvature radius of 0.25 m. The control strategy ensures a range of maneuverability for the robotic artifact despite its underactuated design. The bioinspired solution enables design changes to improve performances without changing the control strategy. The robot can adopt different configurations according to the tasks required. The biomimetics and the carangiform swimming mode are less invasive choices for the marine ecosystem. We believe that our solution is effective, reliable, and sustainable for environmental monitoring, discovery, and animal-robot interaction.

6 Future Work

In the future, the integration of a buoyancy control system into the swimming robot will be evaluated. The focus is to develop a sustainable and robust system that maintains the underactuation, modularity, and biomimetics principles of the design. Initial results show that the proprioceptive control strategy allows for different swimming modes, steering

rates, and speed performances using only one DC motor. To make the proposed solution autonomous and enable it to act in the field, we plan to integrate exteroceptive sensors that can detect environmental parameters and set a reference target in the outside world. For example, an integrated camera in the head of the robotic fish could track a target organism, detect environmental or species anomalies, and analyze animal behavior using artificial intelligence techniques. Bioinspired robots have potential applications in aquafarming, where the biomimetic design and quiet locomotion can reduce stress on monitored marine species. The proposed robot could monitor the environment, detect harmful elements such as pathogens and help preserve the health and welfare of animals, as well as interact with marine species.

Supplementary Information The online version contains supplementary material available at https://doi.org/10.1007/s10846-024-02080-9.

Acknowledgements The authors are grateful to the communal swimming pool of Pontedera staff for having made available their own spaces to do the experiments. The authors also thank Ms. Gloria Bianco and Mr. Raffaele Piciché for their assistance during the tests and their graphic support, and Mr. Luca Padovani for the useful discussion on theoretical aspects of fluid dynamics.

Author Contributions Conceptualization: G.M., and D.R.; methodology: G.M. D.R. and C.S.; formal analysis: G.M., G.S., M.M., G.V., P.D., C.S., D.R.; investigation G.M., G.S., M.M., G.V.; resources: P.D., C.S., D.R.; data curation: G.M., D.R., C.S.; original draft: G.M.; review and editing: G.M., G.S., M.M., G.V., P.D., C.S., D.R.; supervision: D.R.

Funding Open access funding provided by Scuola Superiore Sant'Anna within the CRUI-CARE Agreement. This research was carried out in the framework of the EU H2020-MSCA-RISE-2018 ECOBOTICS.SEA Bio-inspired Technologies for a Sustainable Marine Ecosystem [824043], and the EU H2020 FETOPEN Project 'Robocoenosis - ROBOts in cooperation with a bioCOENOSIS' [899520]. Funders had no role in the study design, data collection and analysis, decision to publish, or preparation of the manuscript.

Availability of Data and Materials Data collected during experimental tests can be made available on request.

Code Availability The code used to analyse and plot the experimental results can be made available on request.

Declarations

Competing Interests The authors declare that they have no financial interests.

Conflict of Interest The authors declare that they have no conflict of interest.

References

1. Mayer, L., Jakobsson, M., Allen, G., Dorschel, B., Falconer, R., Ferrini, V., Lamarche, G., Snaith, H., Weatherall, P.: The nippon foundation-gebco seabed 2030 project: the quest to see the world's oceans completely mapped by 2030. Geosciences **8**(2), 63 (2018). https://doi.org/10.3390/geosciences8020063
2. Halpern, B.S., Frazier, M., Afflerbach, J., Lowndes, J.S., Micheli, F., O'Hara, C., Scarborough, C., Selkoe, K.A.: Recent pace of change in human impact on the world's ocean. Scientific Reports 9(1), 1–8 (2019). https://doi.org/10.1038/s41598-019-47201-9
3. Borrelle, S.B., Rochman, C.M., Liboiron, M., Bond, A.L., Lusher, A., Bradshaw, H., Provencher, J.F.: Opinion: Why we need an international agreement on marine plastic pollution. Proc. Natl. Acad. Sci. **114**(38), 9994–9997 (2017). https://doi.org/10.1073/pnas.1714450114
4. Gu, X., Wang, Z., Wang, J., Ouyang, W., Wang, B., Xin, M., Lian, M., Lu, S., Lin, C., He, M., et al.: Sources, trophodynamics, contamination and risk assessment of toxic metals in a coastal ecosystem by using a receptor model and Monte Carlo simulation. J. Hazard. Mater. **424**, 127482 (2022). https://doi.org/10.1016/j.jhazmat.2021.127482
5. Williams, G., Maksym, T., Wilkinson, J., Kunz, C., Murphy, C., Kimball, P., Singh, H.: Thick and deformed antarctic sea ice mapped with autonomous underwater vehicles. Nat. Geosci. **8**(1), 61–67 (2015). https://doi.org/10.1038/ngeo2299
6. Whitcomb, L.L., Jakuba, M.V., Kinsey, J.C., Martin, S.C., Webster, S.E., Howland, J.C., Taylor, C.L., Gomez-Ibanez, D., Yoerger, D.R.: Navigation and control of the nereus hybrid underwater vehicle for global ocean science to 10,903 m depth: preliminary results. In: 2010 IEEE International Conference on Robotics and Automation, IEEE, pp. 594–600 (2010). https://doi.org/10.1109/ROBOT.2010.5509265
7. Monk, S.A., Schaap, A., Hanz, R., Borisov, S.M., Loucaides, S., Arundell, M., Papadimitriou, S., Walk, J., Tong, D., Wyatt, J., et al.: Detecting and mapping a co2 plume with novel autonomous ph sensors on an underwater vehicle. Int. J. Greenhouse Gas Control **112**, 103477 (2021). https://doi.org/10.1016/j.ijggc.2021.103477
8. Zhong, Q., Zhu, J., Fish, F., Kerr, S., Downs, A., Bart-Smith, H., Quinn, D.: Tunable stiffness enables fast and efficient swimming in fish-like robots. Sci. Robot. **6**(57), 4088 (2021). https://doi.org/10.1126/scirobotics.abe4088
9. Rossi, C., Colorado, J., Coral, W., Barrientos, A.: Bending continuous structures with smas: a novel robotic fish design. Bioinspiration & Biomimetics **6**(4), 045005 (2011). https://doi.org/10.1088/1748-3182/6/4/045005
10. Tytell, E.D., Long, J.H., Jr.: Biorobotic insights into neuromechanical coordination of undulatory swimming. Sci. Robot. **6**(57), 0620 (2021). https://doi.org/10.1126/scirobotics.abk0620
11. Manfredi, L., Assaf, T., Mintchev, S., Marrazza, S., Capantini, L., Orofino, S., Ascari, L., Grillner, S., Wallén, P., Ekeberg, Ö., et al.: A bioinspired autonomous swimming robot as a tool for studying goal-directed locomotion. Biol. Cybern. **107**(5), 513–527 (2013). https://doi.org/10.1007/s00422-013-0566-2

12. Kopman, V., Laut, J., Polverino, G., Porfiri, M.: Closed-loop control of zebrafish response using a bioinspired robotic-fish in a preference test. J. R. Soc. Interface **10**(78), 20120540 (2013). https://doi.org/10.1098/rsif.2012.0540
13. Romano, D., Donati, E., Benelli, G., Stefanini, C.: A review on animal-robot interaction: from bio-hybrid organisms to mixed societies. Biol. Cybern. **113**(3), 201–225 (2019). https://doi.org/10.1007/s00422-018-0787-5
14. Polverino, G., Phamduy, P., Porfiri, M.: Fish and robots swimming together in a water tunnel: robot color and tail-beat frequency influence fish behavior. PLoS ONE **8**(10), 77589 (2013). https://doi.org/10.1371/journal.pone.0077589
15. Porfiri, M.: Inferring causal relationships in zebrafish-robot interactions through transfer entropy: a small lure to catch a big fish. Anim. Behav. Cogn. **5**(4), 341–367 (2018). https://doi.org/10.26451/abc.05.04.03.2018
16. Polverino, G., Karakaya, M., Spinello, C., Soman, V.R., Porfiri, M.: Behavioural and life-history responses of mosquitofish to biologically inspired and interactive robotic predators. J. R. Soc. Interface **16**(158), 20190359 (2019). https://doi.org/10.1098/rsif.2019.0359
17. Romano, D., Stefanini, C.: Individual neon tetras (paracheirodon innesi, myers) optimise their position in the group depending on external selective contexts: lesson learned from a fish-robot hybrid school. Biosyst. Eng. **204**, 170–180 (2021). https://doi.org/10.1016/j.biosystemseng.2021.01.021
18. Stefanini, C., Orlandi, G., Menciassi, A., Ravier, Y., La Spina, G., Grillner, S., Dario, P.: A mechanism for biomimetic actuation in lamprey-like robots. In: The First IEEE/RAS-EMBS International Conference on Biomedical Robotics and Biomechatronics, 2006. BioRob 2006., IEEE, pp. 579–584 (2006). https://doi.org/10.1109/BIOROB.2006.1639151
19. Stefanini, C., Orofino, S., Manfredi, L., Mintchev, S., Marrazza, S., Assaf, T., Capantini, L., Sinibaldi, E., Grillner, S., Wallén, P., et al.: A novel autonomous, bioinspired swimming robot developed by neuroscientists and bioengineers. Bioinspiration & Biomimetics **7**(2), 025001 (2012). https://doi.org/10.1088/1748-3182/7/2/025001
20. Liu, W., Li, F., Stefanini, C., Chen, D., Dario, P.: Biomimetic flexible/compliant sensors for a soft-body lamprey-like robot. Robot. Auton. Syst. **58**(10), 1138–1148 (2010). https://doi.org/10.1016/j.robot.2010.06.006
21. Ikeda, M., Mikuriya, K., Watanabe, K., Hikasa, S., Hamano, Y., Nagai, I.: Influence on the propulsive performance due to the difference in the fin shape of a robotic manta. Artificial Life and Robotics **22**(2), 276–282 (2017). https://doi.org/10.1007/s10015-017-0351-8
22. Chew, C.-M., Lim, Q.-Y., Yeo, K.S.: Development of propulsion mechanism for robot manta ray. In: 2015 IEEE International Conference on Robotics and Biomimetics (ROBIO), pp. 1918–1923 (2015). https://doi.org/10.1109/ROBIO.2015.7419053
23. Kim, E., Youm, Y.: Design and dynamic analysis of fish robot: Potuna. In: IEEE International Conference on Robotics and Automation, 2004. Proceedings. ICRA '04. 2004, vol. 5, pp. 4887–48925 (2004). https://doi.org/10.1109/ROBOT.2004.1302492
24. Farideddin Masoomi, S., Gutschmidt, S., Chen, X., Sellier, M.: The kinematics and dynamics of undulatory motion of a tuna-mimetic robot. Int. J. Adv. Rob. Syst. **12**(7), 83 (2015). https://doi.org/10.5772/60059
25. Chen, Z., Shatara, S., Tan, X.: Modeling of biomimetic robotic fish propelled by an ionic polymer-metal composite caudal fin. IEEE/ASME Trans. Mechatron. **15**(3), 448–459 (2010). https://doi.org/10.1109/TMECH.2009.2027812
26. Kumph, J.M.: Maneuvering of a robotic pike. PhD thesis, Massachusetts Institute of Technology (2000)
27. Yu, J., Zhang, C., Liu, L.: Design and control of a single-motor-actuated robotic fish capable of fast swimming and maneuverability. IEEE/ASME Trans. Mechatron. **21**(3), 1711–1719 (2016). https://doi.org/10.1109/TMECH.2016.2517931
28. Romano, D., Wahi, A., Miraglia, M., Stefanini, C.: Development of a novel underactuated robotic fish with magnetic transmission system. Machines **10**(9), 755 (2022). https://doi.org/10.3390/machines10090755
29. Grillner, S.: The motor infrastructure: from ion channels to neuronal networks. Nat. Rev. Neurosci. **4**(7), 573–586 (2003). https://doi.org/10.1038/nrn1137
30. Grillner, S.: Biological pattern generation: the cellular and computational logic of networks in motion. Neuron **52**(5), 751–766 (2006). https://doi.org/10.1016/j.neuron.2006.11.008
31. Yu, J., Zhang, C., Liu, L.: Design and control of a single-motor-actuated robotic fish capable of fast swimming and maneuverability. IEEE/ASME Trans. Mechatron. **21**(3), 1711–1719 (2016). https://doi.org/10.1109/TMECH.2016.2517931
32. Li, Z., Zhong, Y., Du, R.: A novel underactuated wire-driven robot fish with vector propulsion. In: 2013 IEEE/RSJ International Conference on Intelligent Robots and Systems, pp. 941–946 (2013). https://doi.org/10.1109/IROS.2013.6696463
33. Zhang, P., Wu, Z., Meng, Y., Tan, M., Yu, J.: Nonlinear model predictive position control for a tail-actuated robotic fish. Nonlinear Dyn. **101**(4), 2235–2247 (2020). https://doi.org/10.1007/s11071-020-05963-2
34. Xie, F., Zhong, Y., Du, R., Li, Z.: Central pattern generator (cpg) control of a biomimetic robot fish for multimodal swimming. J. Bionic Eng. **16**(2), 222–234 (2019). https://doi.org/10.1007/s42235-019-0019-2
35. Crespi, A., Lachat, D., Pasquier, A., Ijspeert, A.J.: Controlling swimming and crawling in a fish robot using a central pattern generator. Auton. Robot. **25**(1), 3–13 (2008). https://doi.org/10.1007/s10514-007-9071-6
36. Grillner, S.: Neurobiological bases of rhythmic motor acts in vertebrates. Science **228**(4696), 143–149 (1985). https://doi.org/10.1126/science.3975635
37. Li, L., Liu, D., Deng, J., Lutz, M.J., Xie, G.: Fish can save energy via proprioceptive sensing. Bioinspiration & Biomimetics **16**(5), 056013 (2021). https://doi.org/10.1088/1748-3190/ac165e
38. Sánchez-Rodríguez, J., Celestini, F., Raufaste, C., Argentina, M.: Proprioceptive mechanism for bioinspired fish swimming. Phys. Rev. Lett. **126**, 234501 (2021). https://doi.org/10.1103/PhysRevLett.126.234501
39. Sfakiotakis, M., Lane, D.M., Davies, J.B.C.: Review of fish swimming modes for aquatic locomotion. IEEE J. Oceanic Eng. **24**(2), 237–252 (1999). https://doi.org/10.1109/48.757275
40. Blake, R.W.: Fish functional design and swimming performance. J. Fish Biol. **65**(5), 1193–1222 (2004). https://doi.org/10.1111/j.0022-1112.2004.00568.x
41. Barrett, D., Triantafyllou, M., Yue, D., Grosenbaugh, M., Wolfgang, M.: Drag reduction in fish-like locomotion. J. Fluid Mech. **392**, 183–212 (1999). https://doi.org/10.1017/S0022112099005455
42. Lighthill, M.: Note on the swimming of slender fish. J. Fluid Mech. **9**(2), 305–317 (1960). https://doi.org/10.1017/S0022112060001110
43. Sparenberg, J.: Survey of the mathematical theory of fish locomotion. J. Eng. Math. **44**, 395–448 (2002). https://doi.org/10.1023/A:1021256500244
44. Zhong, Y., Song, J., Yu, H., Du, R.: Toward a transform method from lighthill fish swimming model to biomimetic robot fish. IEEE Robotics and Automation Letters **3**(3), 2632–2639 (2018). https://doi.org/10.1109/LRA.2018.2822310

45. Li, L., Wang, C., Xie, G.: Modeling of a carangiform-like robotic fish for both forward and backward swimming: based on the fixed point. In: 2014 IEEE International Conference on Robotics and Automation (ICRA), pp. 800–805 (2014). https://doi.org/10.1109/ICRA.2014.6906946
46. Chowdhury, A.R., Kumar, V., Prasad, B., Kumar, R., Panda, S.K.: Kinematic study and implementation of a bio-inspired robotic fish underwater vehicle in a lighthill mathematical framework. Robotics and Biomimetics **1**, 1–16 (2014). https://doi.org/10.1186/s40638-014-0015-2
47. Wang, J., Tan, X.: A dynamic model for tail-actuated robotic fish with drag coefficient adaptation. Mechatronics **23**(6), 659–668 (2013). https://doi.org/10.1016/j.mechatronics.2013.07.005
48. Weerasooriya, S., El-Sharkawi, M.A.: Identification and control of a dc motor using back-propagation neural networks. IEEE Trans. Energy Convers. **6**(4), 663–669 (1991). https://doi.org/10.1109/60.103639
49. Yu, J., Tan, M., Chen, J., Zhang, J.: A survey on cpg-inspired control models and system implementation. IEEE Transactions on Neural Networks and Learning Systems **25**(3), 441–456 (2014). https://doi.org/10.1109/TNNLS.2013.2280596
50. Pearson, K.G.: Proprioceptive regulation of locomotion. Curr. Opin. Neurobiol. **5**(6), 786–791 (1995). https://doi.org/10.1016/0959-4388(95)80107-3
51. Ryczko, D., Simon, A., Ijspeert, A.J.: Walking with salamanders: from molecules to biorobotics. Trends Neurosci. **43**(11), 916–930 (2020). https://doi.org/10.1016/j.tins.2020.08.006
52. Romano, D., Stefanini, C.: Robot-fish interaction helps to trigger social buffering in neon tetras: the potential role of social robotics in treating anxiety. Int. J. Soc. Robot. **14**(4), 963–972 (2022). https://doi.org/10.1007/s12369-021-00829-y
53. Bonnet, F., Cazenille, L., Séguret, A., Gribovskiy, A., Collignon, B., Halloy, J., Mondada, F.: Design of a modular robotic system that mimics small fish locomotion and body movements for ethological studies. International Journal of Advanced Robotic Systems **14**(3) (2017). https://doi.org/10.1177/1729881417706628
54. Ming, A., Park, S., Nagata, Y., Shimojo, M.: Development of underwater robots using piezoelectric fiber composite. In: 2009 IEEE International Conference on Robotics and Automation, pp. 3821–3826 (2009). https://doi.org/10.1109/ROBOT.2009.5152723
55. Nguyen, Q., Heo, S., Park, H., Byun, D.: Performance evaluation of an improved fish robot actuated by piezoceramic actuators. Smart Mater. Struct. **19**(3), 035030 (2010). https://doi.org/10.1088/0964-1726/19/3/035030
56. Zhong, Y., Li, Z., Du, R.: A novel robot fish with wire-driven active body and compliant tail. IEEE/ASME Trans. Mechatron. **22**(4), 1633–1643 (2017). https://doi.org/10.1109/TMECH.2017.2712820
57. Zhong, Y., Song, J., Yu, H., Du, R.: Toward a transform method from lighthill fish swimming model to biomimetic robot fish. IEEE Robotics and Automation Letters **3**(3), 2632–2639 (2018). https://doi.org/10.1109/LRA.2018.2822310
58. Chen, J., Yin, B., Wang, C., Xie, F., Du, R., Zhong, Y.: Bioinspired closed-loop cpg-based control of a robot fish for obstacle avoidance and direction tracking. J. Bionic Eng. **18**(1), 171–183 (2021). https://doi.org/10.1007/s42235-021-0008-0
59. Yu, J., Liu, L., Wang, L., Tan, M., Xu, D.: Turning control of a multilink biomimetic robotic fish. IEEE Trans. Rob. **24**(1), 201–206 (2008). https://doi.org/10.1109/TRO.2007.914850
60. Liu, J., Hu, H.: Biological inspiration: from carangiform fish to multi-joint robotic fish. J. Bionic Eng. **7**(1), 35–48 (2010). https://doi.org/10.1016/S1672-6529(09)60184-0
61. Bal, C., Koca, G.O., Korkmaz, D., Akpolat, Z.H., Ay, M.: Cpg-based autonomous swimming control for multi-tasks of a biomimetic robotic fish. Ocean Eng. **189**, 106334 (2019). https://doi.org/10.1016/j.oceaneng.2019.106334
62. Rao, D., Kamat, H.: Neuro-fuzzy system for robotics applications. IETE J. Res. **42**(4–5), 325–333 (1996). https://doi.org/10.1080/03772063.1996.11415938
63. Naveen, C., Meenakshipriya, B., Tony Thomas, A., Sathiyavathi, S., Sathishbabu, S.: Real-time implementation of iterative learning control for an electro-hydraulic servo system. IETE J. Res. **69**(2), 649–664 (2023). https://doi.org/10.1080/03772063.2022.2069164
64. El Hamidi, K., Mjahed, M., El Kari, A., Ayad, H., El Gmili, N.: Design of hybrid neural controller for nonlinear mimo system based on narma-l2 model. IETE J. Res. **69**(5), 3038–3051 (2023). https://doi.org/10.1080/03772063.2021.1909507
65. Zhuang, Z., Tao, H., Chen, Y., Stojanovic, V., Paszke, W.: An optimal iterative learning control approach for linear systems with nonuniform trial lengths under input constraints. IEEE Transactions on Systems, Man, and Cybernetics: Systems (2022). https://doi.org/10.1109/TSMC.2022.3225381
66. Zhang, Z., Song, X., Sun, X., Stojanovic, V.: Hybrid-driven-based fuzzy secure filtering for nonlinear parabolic partial differential equation systems with cyber attacks. Int. J. Adapt. Control Signal Process. **37**(2), 380–398 (2023). https://doi.org/10.1002/acs.3529
67. Song, X., Wu, C., Stojanovic, V., Song, S.: 1 bit encoding-decoding-based event-triggered fixed-time adaptive control for unmanned surface vehicle with guaranteed tracking performance. Control. Eng. Pract. **135**, 105513 (2023). https://doi.org/10.1016/j.conengprac.2023.105513
68. Stojanović, V.: Fault-tolerant control of a hydraulic servo actuator via adaptive dynamic programming. Mathematical Modelling and Control (2023). https://doi.org/10.3934/mmc.2023016
69. Polverino, G., Abaid, N., Kopman, V., Macrì, S., Porfiri, M.: Zebrafish response to robotic fish: preference experiments on isolated individuals and small shoals. Bioinspiration & Biomimetics **7**(3), 036019 (2012). https://doi.org/10.1088/1748-3182/7/3/036019
70. Romano, D., Stefanini, C.: Unveiling social distancing mechanisms via a fish-robot hybrid interaction. Biol. Cybern. **115**(6), 565–573 (2021). https://doi.org/10.1007/s00422-021-00867-9
71. Bonnet, F., Kato, Y., Halloy, J., Mondada, F.: Infiltrating the zebrafish swarm: design, implementation and experimental tests of a miniature robotic fish lure for fish-robot interaction studies. Artificial Life and Robotics **21**, 239–246 (2016). https://doi.org/10.1007/s10015-016-0291-8
72. Butail, S., Polverino, G., Phamduy, P., Del Sette, F., Porfiri, M.: Influence of robotic shoal size, configuration, and activity on zebrafish behavior in a free-swimming environment. Behav. Brain Res. **275**, 269–280 (2014). https://doi.org/10.1016/j.bbr.2014.09.015

Gianluca Manduca [M.Sc. in Automation and Control Eng.] is a PhD student at The BioRobotics Institute of Scuola Superiore Sant'Anna of Pisa. Gianluca graduated in Automation and Control Engineering at Politecnico di Milano; before embarking on his PhD path, he spent a period as a visiting scholar at the Center for Automotive Research (CAR) of The Ohio State University, Columbus, OH, USA. The background in automation and control formed during studies initially contributed to the automotive sector, with work related to autonomous driving and lithium-ion battery modeling. Currently, Gianluca deals with biorobotic systems and biosensors managed through artificial intelligence techniques, with application to underwater robots and environmental monitoring. He is involved in several national and international research projects.

Gaspare Santaera [B.Sc. in Electronic Eng. and M.Sc. in Automation Eng.] is a PhD student at The BioRobotics Institute of Scuola Superiore Sant'Anna of Pisa. He started his career as research fellow at the Research Center "E. Piaggio" of the University of Pisa in 2013, working on the design and the control of robotic and prosthetics hands. In 2016, he moved to the Istituto Italiano di Tecnologia (IIT) in Genoa, then he transitioned to the industrial sector in 2019, working at E.P. Elevatori Premontati on electrical design of novel elevators. In March 2020, he joined The BioRobotics Institute of Scuola Sant'Anna of Pisa, where he is currently a PhD student specializing in electronics design for robots. His expertise includes problem-solving, PCB design, and firmware/hardware integration, with a focus on swarm and underwater robotics. He has been involved in several EU projects such as PaCMAN, WearHAP, SoMa, SoftPRo, WalkMAN, Thing, Robocoenosis, Ecobotics.

Marco Miraglia [B.Sc. in Aerospace Eng. (honors), M.Sc. in Aeronautical Eng. (honors), PhD in BioRobotics (honors)] has specialized in biomimetic and industrial robotics during his research activities at The BioRobotics Institute of Scuola Superiore Sant'Anna of Pisa. He contributed to the development of Finite Element Method (FEM) models and mechanical designs throughout his activities. He held the position of mechanical designer at IUVO S.r.l., where he contributed to industrial automation projects. He later transitioned to ESA S.p.A..

Godfried Jansen Van Vuuren received his senior certificate from Vredenburg High in 2004. He worked in the construction industry for 7 years as an electrical technician, where he engaged himself in the installation and maintenance of backup generator systems and industrial cooling systems for multi-story office buildings. He started at Scuola Superiore Sant'Anna in 2012 as lab technician and worked on various European projects including Angels, Replicator, CoCoRo, subCULTron and Robocoenosis. His main responsibilities include design, fabrication, assembly, testing and maintenance of various autonomous robotic platforms within the above-mentioned projects.

Paolo Dario is Emeritus Professor at Scuola Superiore Sant'Anna in Pisa. Until 2021, he was Full Professor of Biomedical Robotics and taught courses to PhD students in The BioRobotics Doctoral Program and to students in the Bionics Engineering Course, jointly organized by the University of Pisa and Scuola Superiore Sant'Anna. He served as Director and Founder (2011- 2017) of The BioRobotics Institute, Coordinator and Founder of The BioRobotics Doctoral Program at the Scuola Superiore Sant'Anna. He was coordinator of the doctoral program until 2019. He served as Pro-Rector for Innovation, Knowledge Transfer, and Third Mission at the University and Coordinator of the Department of Excellence in Robotics and AI at Scuola Superiore Sant'Anna. He is Scientific Director of the ARTES4.0 Competence Center on Industry 4.0, co-financed by the Ministry of Economic Development (MiSE) and involving 127 partners (public and private). He has also been a member of university councils, national and international evaluation committees for research and academic activities, and numerous national and international advisory boards for assessing candidates for academic positions. Paolo Dario served as President of the IEEE Robotics and Automation Society from 2002 to 2003. He has been General or Program Chair of numerous major international conferences, including IEEE ICAR, ICRA, IROS, and BioRob, which he founded. He is an IEEE Life Fellow, a member of the European Society on Medical and Biological Engineering, and he has received numerous awards and honors.

Cesare Stefanini [M.Sc. in Mech. Eng. (honors), PhD in Microengineering (honors)] is Full Professor of Bioengineering at The BioRobotics Institute of Scuola Superiore Sant'Anna of Pisa, Italy, with the role of Institute Director and Area Leader in "Creative Engineering Design". His research activity is applied to different fields, including biomechatronics, and micromechatronics for medical and industrial applications. He received international recognitions for the development of novel actuators for microrobots and he has been visiting researcher at the University of Stanford, Center for Design Research, and Professor at Khalifa University, UAE.

Donato Romano [M.Sc. in Agriculture Science and Technologies (honors), PhD in BioRobotics (honors)] is currently Assistant Professor at The BioRobotics Institute of Scuola Superiore Sant'Anna of Pisa, Italy, where he coordinates the Biorobotic Ecosystems Laboratory. Romano is mainly focusing his activities on bioinspired and biomimetic robotics, and in particular on animal-robot interaction, biohybrid systems, natural and biohybrid intelligence, ethorobotics, neuroethology. Romano received national and international recognitions for his research. He also has been visiting researcher at Khalifa University, Abu Dhabi (UAE). He is Member of the Editorial Board for many International Scientific Journals. Romano is Coordinator, PI, or partner of several national and international research projects.

Authors and Affiliations

Gianluca Manduca[1,2] · Gaspare Santaera[1,2] · Marco Miraglia[1,2] · Godfried Jansen Van Vuuren[1,2] · Paolo Dario[1,2] · Cesare Stefanini[1,2] · Donato Romano[1,2]

Gaspare Santaera
gaspare.santaera@santannapisa.it

Marco Miraglia
marco.miraglia@santannapisa.it

Godfried Jansen Van Vuuren
godfried.jansenvanvuuren@santannapisa.it

Paolo Dario
paolo.dario@santannapisa.it

Cesare Stefanini
cesare.stefanini@santannapisa.it

[1] The BioRobotics Institute, Scuola Superiore Sant'Anna, Viale R. Piaggio 34, Pontedera (PI) 56025, Italy

[2] Department of Excellence in Robotics and AI, Scuola Superiore Sant'Anna, Piazza Martiri della Libertà 33, Pisa (PI) 56127, Italy